LiDAR and True-color Orthophotographs:
Snohomish River Estuary, WA
November 30, 2009

Revision 2
(from October 23, 2009 report)

Submitted to:

Diana Martinez
Puget Sound Regional Council
1011 Western Ave
Suite 500
Seattle, WA 98104-1035

Submitted by:

Watershed Sciences
257B SW Madison Ave.
Corvallis, OR 97333

529 SW 3rd Ave. Suite 300
Portland, Oregon 97204

WatershedSciences

LiDAR and True-color Orthophotographs
AIRBORNE DATA ACQUISITION AND PROCESSING:
Snohomish River Estuary, WA

TABLE OF CONTENTS

1. Overview

Watershed Sciences, Inc. (WS) co-aquired Light Detection and Ranging (LiDAR) data and True-color Orthophotographs of the Snohomish River Estuary, WA on July 20 & 21, 2009. The original requested survey area (26,150 acres) was expanded, at the client's request, to include more of the valley lowland areas in the SW and SE edge of the original AOI as well as additional creeks on the northern edge of the survey (**Figure 1**). The total area of delivered LiDAR and True-color Orthophotographs, including the expansion and 100 m buffer, is 32,140 acres.

Figure 1. Snohomish River Estuary River Project survey area
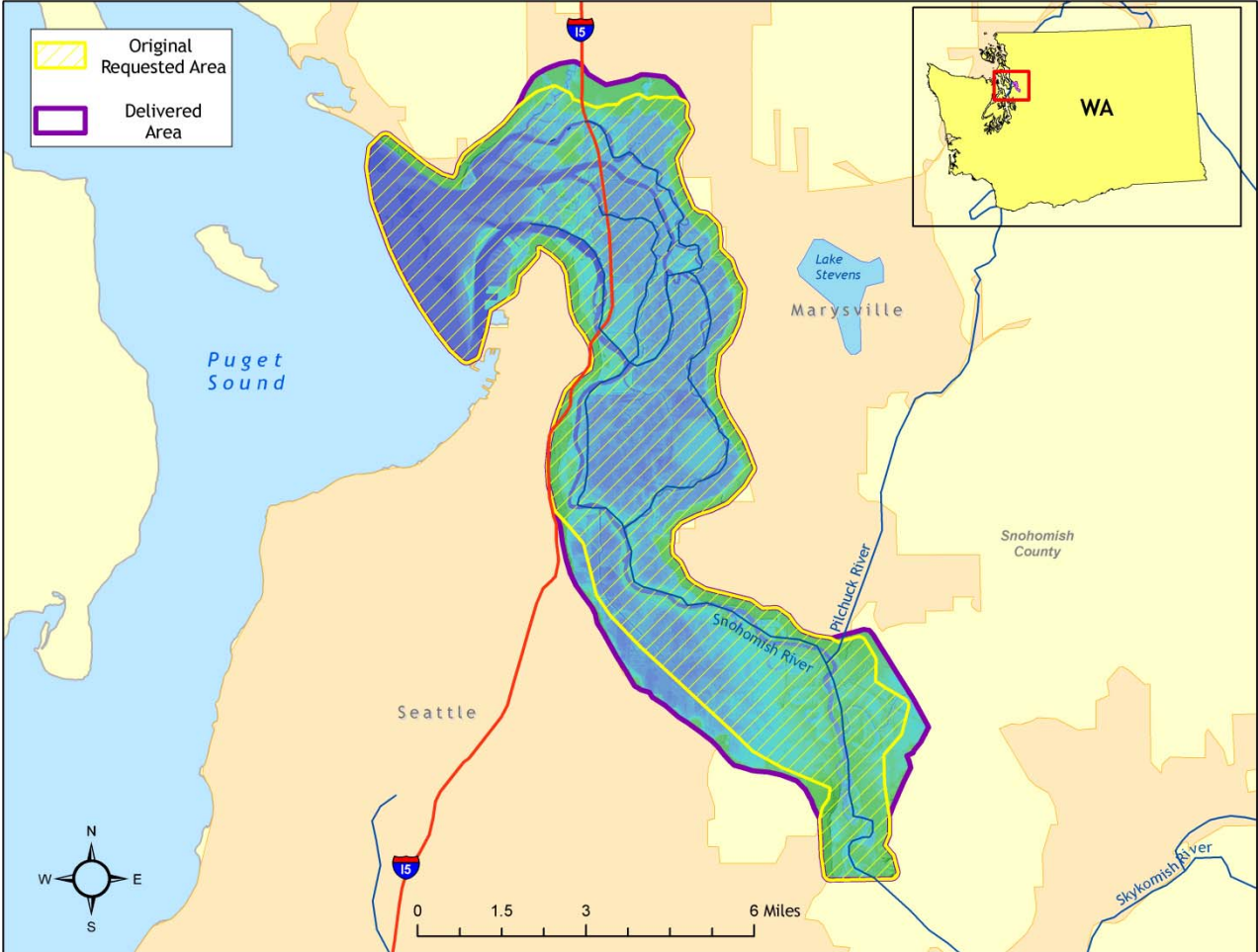
2. Acquisition

2.1 Airborne Survey – Instrumentation and Methods

The LiDAR survey uses a Leica ALS50 Phase II laser system. For the Snohomish River Estuary survey site, the sensor scan angle was ±12° from nadir[1] with a pulse rate designed to yield an average native density (number of pulses emitted by the laser system) of ≥ 8 points per square meter over terrestrial surfaces. All survey areas were surveyed with an opposing flight line side-lap of ≥50% (≥100% overlap) to reduce laser shadowing and increase surface laser painting. The Leica ALS50 Phase II system allows up to four range measurements (returns) per pulse, and all discernable laser returns were processed for the output dataset. It is not uncommon for some types of surfaces (e.g. dense vegetation or water) to return fewer pulses than the laser originally emitted. These discrepancies between 'native' and 'delivered' density will vary depending on terrain, land cover and the prevalence of water bodies.

The image acquisition uses a Leica RCD105 medium format camera. The RCD105 has a 39 mega-pixel CCD array with a 60 mm focal lens and 45° field of view (FOV). All study areas were surveyed with an along line overlap of ≥60% and a between line sidelap of ≥30% to ensure complete coverage

To accurately solve for laser point position (geographic coordinates x, y, z), the positional coordinates of the airborne sensor and the attitude of the aircraft were recorded continuously throughout the LiDAR data collection mission. Aircraft position was measured twice per second (2 Hz) by an onboard differential GPS unit. Aircraft attitude was measured 200 times per second (200 Hz) as pitch, roll and yaw (heading) from an onboard inertial measurement unit (IMU). To allow for post-processing correction and calibration, aircraft/sensor position and attitude data are indexed by GPS time.

The Cessna Caravan is a stable platform, ideal for flying slow and low for high density projects. The Leica ALS50 sensor head installed in the Caravan is shown on the left.

---

[1] Nadir refers to the perpendicular vector to the ground directly below the aircraft. Nadir is commonly used to measure the angle from the vector and is referred to a "degrees from nadir".

LiDAR Data Acquisition and Processing: Snohomish River Estuary, WA

Prepared by Watershed Sciences, Inc.

2.2 Ground Survey – Instrumentation and Methods

The following ground survey data were collected to enable the geo-spatial correction of the aircraft positional coordinate data collected throughout the flight, and to allow for quality assurance checks on final LiDAR data products.

2.2.1 Survey Control

Simultaneous with the airborne data collection mission, we conducted multiple static (1 Hz recording frequency) ground surveys over monuments with known coordinates (**Table 1)**. Indexed by time, these GPS data are used to correct the continuous onboard measurements of aircraft position recorded throughout the mission. Multiple sessions were processed over the same monument to confirm antenna height measurements and reported position accuracy. After the airborne survey, these static GPS data were then processed using triangulation with Continuously Operating Reference Stations (CORS) stations, and checked against the Online Positioning User Service (OPUS[2]) to quantify daily variance. Controls were located within 13 nautical miles of the mission area(s).

Trimble GPS survey equipment configured for collecting RTK data.

---

[2] Online Positioning User Service (OPUS) is run by the National Geodetic Survey to process corrected monument positions.

LiDAR Data Acquisition and Processing: Snohomish River Estuary, WA

Prepared by Watershed Sciences, Inc.

Table 1. Base Station Survey Control coordinates for the Snohomish survey area.

| Base Station ID | Datum: NAD83 (CORS91) | | GRS80 |
	Latitude	Longitude	Ellipsoid Z (meters)
SHO_RT1	47° 58′ 40.335″	122° 9′ 29.620″	-21.234
SHO_RT2	47° 58′ 40.255″	122° 9′ 39.059″	-21.518

Table 2. Dates of acquisition for both LiDAR data and aerial photos.

Area of Interest	LiDAR	Photos
Snohomish River Estuary	July 20 & 21, 2009	July 20 & 21, 2009

2.2.2 RTK Survey

To enable assessment of LiDAR data accuracy, ground truth points were collected using GPS based real-time kinematic (RTK) surveying. For an RTK survey, the ground crew uses a roving unit to receive radio-relayed corrected positional coordinates for all ground points from a GPS base station set up over a survey control monument. Instrumentation includes multiple Trimble DGPS units (R8). RTK surveying allows for precise location measurements with an error (σ) of ≤ 1.5 cm (0.6 in). **Figure 2** below portrays a distribution of hard surface RTK point locations used for the survey areas. Additional RTK surveys were taken by Watershed Sciences (in low grass vegetation) and the client (in high marsh vegetation) to compare absolute accuracy amongst land covers; this data is presented in **Table 4.**

To assess spatial accuracy of the orthophotographs they are compared against control points identified from the LIDAR intensity images. The control points were collected\measured on surface features such as painted road-lines, and boulders in the stream beds. The accuracy of the final mosaic, expressed as root mean square error (RMSE), was calculated in relation to the LiDAR-derived control points. **Figure 3** displays the co-registration between orthorectified photographs and LiDAR intensity images.

LiDAR Data Acquisition and Processing: Snohomish River Estuary, WA

Prepared by Watershed Sciences, Inc.

Figure 2. RTK and base station locations used for the Snohomish survey area.
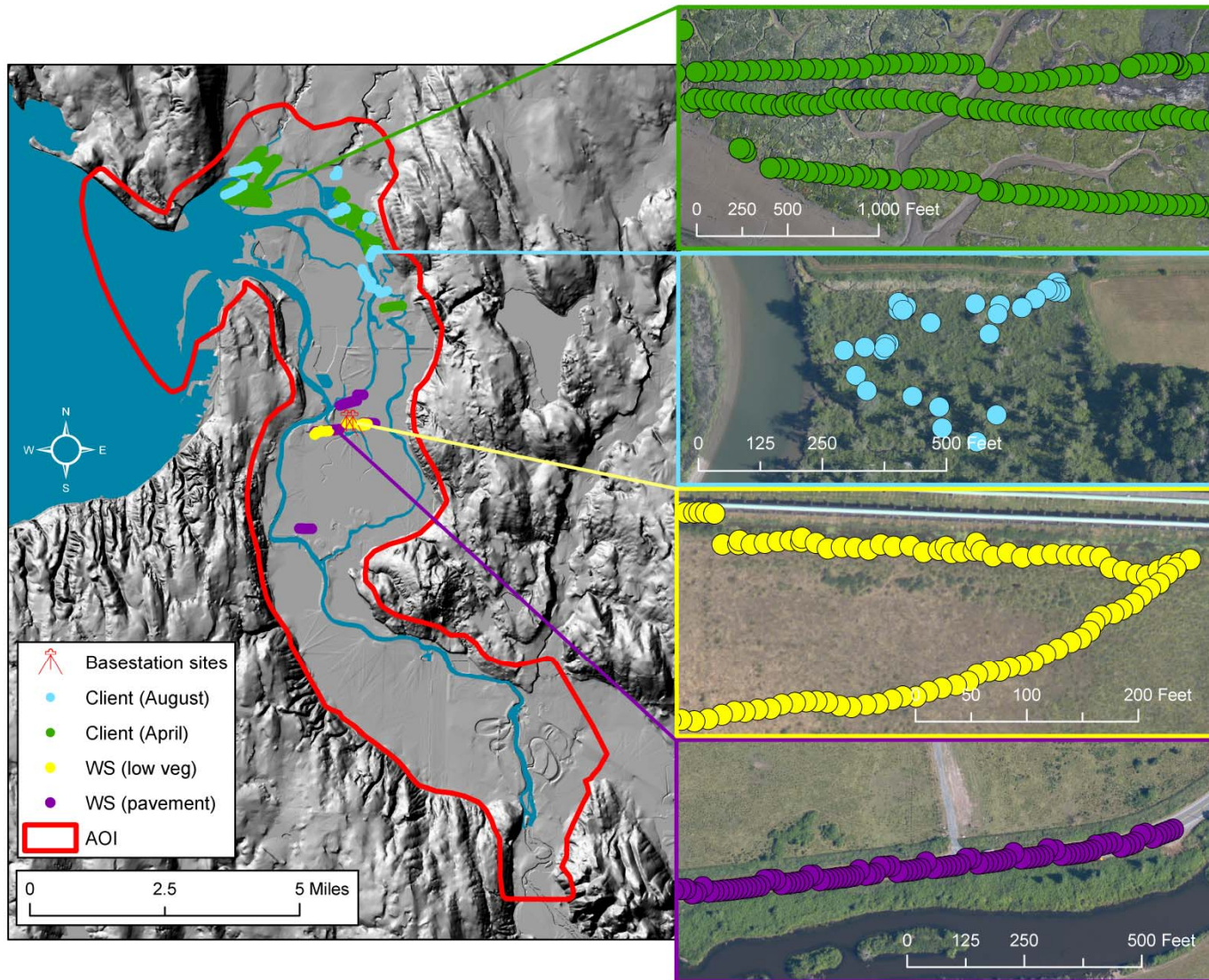
Figure 3. Example of co-registration of color images with LiDAR intensity images
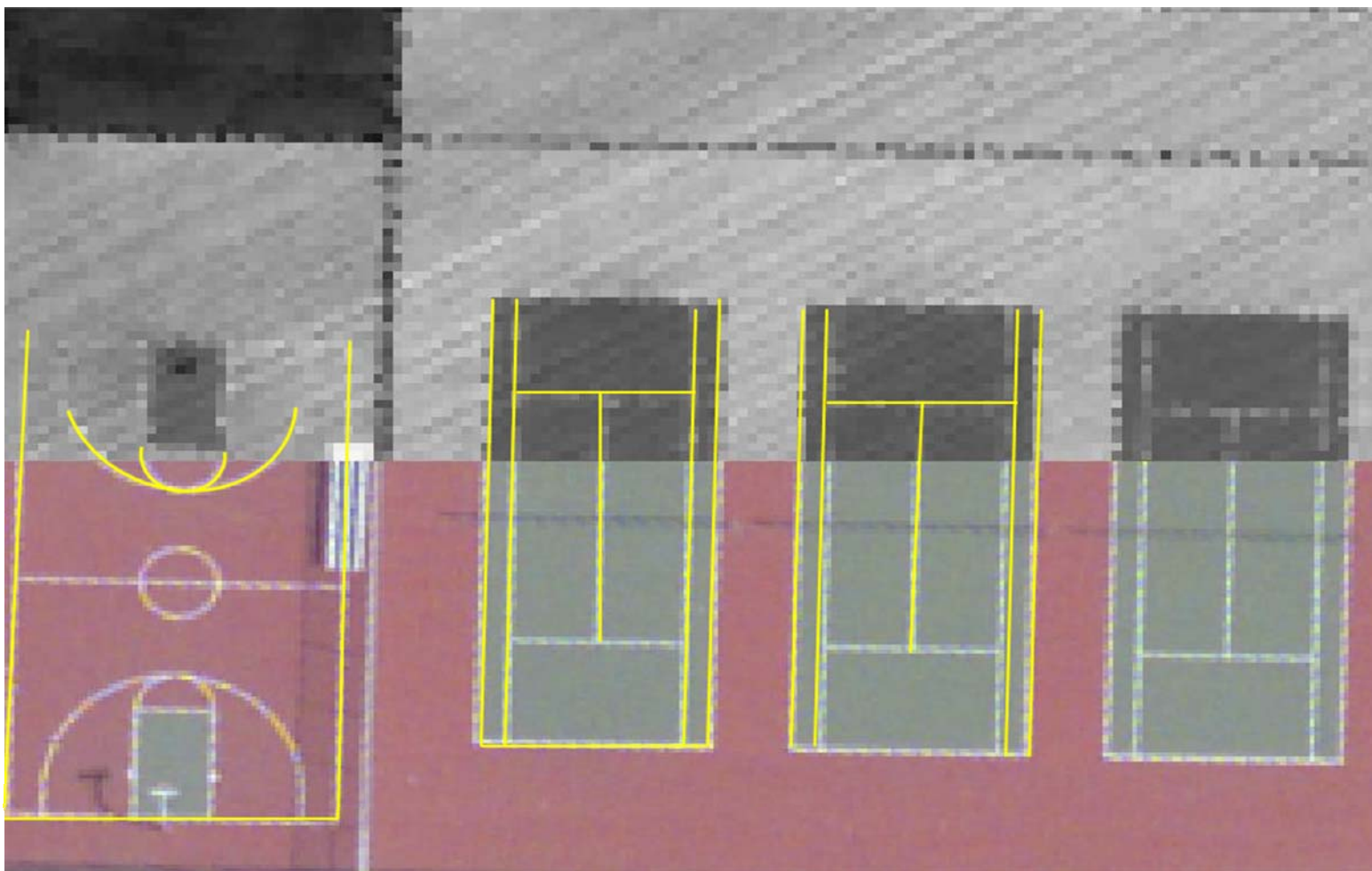
3. Data Processing

3.1 Applications and Work Flow Overview

1. Resolved kinematic corrections for aircraft position data using kinematic aircraft GPS and static ground GPS data.
   Software: Waypoint GPS v.8.10, Trimble Geomatics Office v.1.62

2. Developed a smoothed best estimate of trajectory (SBET) file that blends post-processed aircraft position with attitude data Sensor head position and attitude were calculated throughout the survey. The SBET data were used extensively for laser point processing.
   Software: IPAS v.1.4

3. Calculated laser point position by associating SBET position to each laser point return time, scan angle, intensity, etc. Created raw laser point cloud data for the entire survey in *.las (ASPRS v1.1) format.
   Software: ALS Post Processing Software v.2.69

4. Imported raw laser points into manageable blocks (less than 500 MB) to perform manual relative accuracy calibration and filter for pits/birds. Ground points were then classified for individual flight lines (to be used for relative accuracy testing and calibration).
   Software: TerraScan v.9.001

5. Using ground classified points per each flight line, the relative accuracy was tested. Automated line-to-line calibrations were then performed for system attitude parameters (pitch, roll, heading), mirror flex (scale) and GPS/IMU drift. Calibrations were performed on ground classified points from paired flight lines. Every flight line was used for relative accuracy calibration.
   Software: TerraMatch v.9.001

6. Position and attitude data were imported. Resulting data were classified as ground and non-ground points. Statistical absolute accuracy was assessed via direct comparisons of ground classified points to ground RTK survey data. Data were then converted to orthometric elevations (NAVD88) by applying a Geoid03 correction. Ground models were created as a triangulated surface and exported as ArcInfo ASCII grids at a 1-meter pixel resolution.
   Software: TerraScan v.9.001, ArcMap v9.3, TerraModeler v.9.001

7. Converted raw images to tif format, calibrating raw image pixels for gain and exposure settings of each image.
   Software: Leica Calibration Post Processing v.1.0.4

8. Calculated photo position and orientation by associating the SBET position (Step 3) to each image capture time.
   Software: IPASCO v.1.3

9. Orthorectified calibrated tiffs utilizing photo orientation information (Step 8) and the LiDAR-derived ground surface (Step 6).
   Software: Leica Photogrammetry Suite v.9.2

10. To correct light imbalances between overlapping images, radiometric global tilting adjustments were applied to the rectified images.
    Software: OrthoVista v.4.4.

---

11. The color corrected images were then mosaicked together for the survey area and subset into tiles to make the file size more manageable.

    Software: OrthoVista v.4.4.

12. Mosaicked tiles were inspected for misalignments introduced by automatic seam generation. Misalignments were corrected by manual adjustment to seams.

    Software: Adobe Photoshop 7.0, Ortho Vista 4.4

3.2 Aircraft Kinematic GPS and IMU Data

LiDAR survey datasets were referenced to the 1 Hz static ground GPS data collected over pre-surveyed monuments with known coordinates. While surveying, the aircraft collected 2 Hz kinematic GPS data, and the onboard inertial measurement unit (IMU) collected 200 Hz aircraft attitude data. Leica IPAS Suite was used to process the kinematic corrections for the aircraft. The static and kinematic GPS data were then post-processed after the survey to obtain an accurate GPS solution and aircraft positions. IPAS v.1.4 was used to develop a trajectory file that includes corrected aircraft position and attitude information. The trajectory data for the entire flight survey session were incorporated into a final smoothed best estimated trajectory (SBET) file that contains accurate and continuous aircraft positions and attitudes.

3.3 Laser Point Processing

Laser point coordinates were computed using the IPAS and ALS Post Processor software suites based on independent data from the LiDAR system (pulse time, scan angle), and aircraft trajectory data (SBET). Laser point returns (first through fourth) were assigned an associated (x, y, z) coordinate along with unique intensity values (0-255). The data were output into large LAS v. 1.2 files; each point maintains the corresponding scan angle, return number (echo), intensity, and x, y, z (easting, northing, and elevation) information.

These initial laser point files were too large for subsequent processing. To facilitate laser point processing, bins (polygons) were created to divide the dataset into manageable sizes (< 500 MB). Flightlines and LiDAR data were then reviewed to ensure complete coverage of the survey area and positional accuracy of the laser points.

Laser point data were imported into processing bins in TerraScan, and manual calibration was performed to assess the system offsets for pitch, roll, heading and scale (mirror flex). Using a geometric relationship developed by Watershed Sciences, each of these offsets was resolved and corrected if necessary.

LiDAR points were then filtered for noise, pits (artificial low points) and birds (true birds as well as erroneously high points) by screening for absolute elevation limits, isolated points and height above ground. Each bin was then manually inspected for remaining pits and birds and spurious points were removed. In a bin containing approximately 7.5-9.0 million points, an average of 50-100 points are typically found to be artificially low or high. Common sources of non-terrestrial returns are clouds, birds, vapor, haze, decks, brush piles, etc.

Internal calibration was refined using TerraMatch. Points from overlapping lines were tested for internal consistency and final adjustments were made for system misalignments (i.e., pitch, roll, heading offsets and scale). Automated sensor attitude and scale corrections yielded 3-5 cm improvements in the relative accuracy. Once system misalignments were corrected, vertical GPS drift was then resolved and removed per flight line, yielding a slight improvement (<1 cm) in relative accuracy.

The TerraScan software suite is designed specifically for classifying near-ground points (Soininen, 2004). The processing sequence began by 'removing' all points that were not 'near' the earth based on geometric constraints used to evaluate multi-return points. The resulting bare earth (ground) model was visually inspected and additional ground point modeling was performed in site-specific areas to improve ground detail. This manual editing of grounds often occurs in areas with known ground modeling deficiencies, such as: bedrock outcrops, cliffs, deeply incised stream banks, and dense vegetation. In some cases, automated ground point classification erroneously included known vegetation (i.e., understory, low/dense shrubs, etc.). These points were manually reclassified as non-grounds. Ground surface rasters were developed from triangulated irregular networks (TINs) of ground points.

3.4 Orthophotograph Processing

Image spectral values were calibrated to specific gain and exposure settings associated with each capture using Leica's Calibration Post Processing software. The calibrated images were saved in tiff format to be used as inputs for the rectification process. Photo position and orientation were then calculated by assigning aircraft position and attitude information to each image by associating the time of image capture with trajectory file (SBET) in IPASCO. Photos were then orthorectified to the LiDAR derived ground surface using LPS. This typically results in <2 pixel relative accuracy between images. Relative accuracy can vary slightly with terrain but offsets greater than 2 pixels tend to manifest at the image edges which are typically removed in the mosaic process.

The rectified images were mosaicked together in a three step process using Orthovista. First a color correction was applied to each image using global tilting adjustments designed to homogenize overlapping regions. Second, an automated seam generation process selected the most nadir portion of each image while drawing seams around landscape features such that discrepancies between images was minimized. These images were manually inspected for incongruities between color balance and spatial alignment and then redrawn if necessary to correct these issues. Finally the mosaic was subset into tiles of a manageable size (3000 x 3000 ft) indexed by the coordinates of the upper left corner of each tile.

4. LiDAR Accuracy Assessment

Our LiDAR quality assurance process uses the data from the real-time kinematic (RTK) ground survey conducted in the survey area. In this project, a total of **806 RTK** GPS measurements were collected on hard surfaces distributed among multiple flight swaths. To assess absolute accuracy, we compared the location coordinates of these known RTK ground survey points to those calculated for the closest laser points. As an additional measure of accuracy, RTK

points were collected by Watershed Sciences and the client, in low and high vegetation classes. A comparison of check points against ground classified LiDAR points is summarized by land cover class in **Table 4**.

4.1 Laser Noise and Relative Accuracy

Laser point absolute accuracy is largely a function of laser noise and relative accuracy. To minimize these contributions to absolute error, we first performed a number of noise filtering and calibration procedures prior to evaluating absolute accuracy.

Laser Noise
For any given target, laser noise is the breadth of the data cloud per laser return (i.e., last, first, etc.). Lower intensity surfaces (roads, rooftops, still/calm water) experience higher laser noise. The laser noise range for this survey was approximately 0.02 meters.

Relative Accuracy
Relative accuracy refers to the internal consistency of the data set - the ability to place a laser point in the same location over multiple flight lines, GPS conditions, and aircraft attitudes. Affected by system attitude offsets, scale, and GPS/IMU drift, internal consistency is measured as the divergence between points from different flight lines within an overlapping area. Divergence is most apparent when flight lines are opposing. When the LiDAR system is well calibrated, the line-to-line divergence is low (<10 cm). See Appendix A for further information on sources of error and operational measures that can be taken to improve relative accuracy.

Relative Accuracy Calibration Methodology
1. Manual System Calibration: Calibration procedures for each mission require solving geometric relationships that relate measured swath-to-swath deviations to misalignments of system attitude parameters. Corrected scale, pitch, roll and heading offsets were calculated and applied to resolve misalignments. The raw divergence between lines was computed after the manual calibration was completed and reported for each survey area.
2. Automated Attitude Calibration: All data were tested and calibrated using TerraMatch automated sampling routines. Ground points were classified for each individual flight line and used for line-to-line testing. System misalignment offsets (pitch, roll and heading) and scale were solved for each individual mission and applied to respective mission datasets. The data from each mission were then blended when imported together to form the entire area of interest.
3. Automated Z Calibration: Ground points per line were utilized to calculate the vertical divergence between lines caused by vertical GPS drift. Automated Z calibration was the final step employed for relative accuracy calibration.

4.2 Absolute Accuracy

The vertical accuracy of the LiDAR data is described as the mean and standard deviation (sigma ~ σ) of divergence of LiDAR point coordinates from RTK ground survey point coordinates. To provide a sense of the model predictive power of the dataset, the root mean square error (RMSE) for vertical accuracy is also provided. Statements of statistical accuracy

---

LiDAR Data Acquisition and Processing: Snohomish River Estuary, WA

Prepared by Watershed Sciences, Inc.

apply to fixed terrestrial surfaces only and may not be applied to areas of dense vegetation or steep terrain.

The horizontal accuracy of the final photo mosaic is described by the mean, standard deviation (sigma – σ), and RMSE of divergence of the photo point coordinates (x,y) from the control point coordinates identified from LiDAR intensity images.

These statistics assume the error distributions for x, y, and z are normally distributed, thus we also consider the skew and kurtosis of distributions when evaluating error statistics.

5. Study Area Results

Summary statistics for point resolution and accuracy (relative and absolute) of the LiDAR data collected in the Snohomish River Estuary survey area are presented below in terms of central tendency, variation around the mean, and the spatial distribution of the data (for point resolution by bin). Summary statistics for the True-color Orthophotographs including resolution and horizontal accuracy are also presented below.

5.1 LiDAR Data Summary

Table 3. Resolution and Accuracy - Specifications and Achieved Values

	Targeted	**Achieved**
Resolution:	$\geq$ 8 points/m^2	6.97 points/m^2 (0.64 points/ft^2)
*Vertical Accuracy (1 σ):	<15 cm	3 cm (0.097 ft)

* Based on 806 hard-surface control points

5.2 LiDAR Data Density/Resolution

The first return laser point density of 6.97 points/m^2 was slightly below the targeted density of 8 points/m^2 (**Table 3**). Some types of surfaces (i.e., dense vegetation, breaks in terrain, steep slopes, water) may return fewer pulses (delivered density) than the laser originally emitted (native density). Because the Snohomish survey area included a large proportion of water, some areas had a lower native return density (**Figure 6**). In addition, the expanded boundary areas were covered only by the last peripheral flight lines overlying the project area, with no overlap. Single coverage areas at the AOI edge are normally truncated from the delivered AOI because LiDAR point densities are lower.

Ground classifications were derived from automated ground surface modeling and manual, supervised classifications where it was determined that the automated model had failed. Ground return densities will be lower in areas of dense vegetation, water, or buildings. The ground-classified point map in **Figure 7** identifies these areas of lower ground return densities.

Data Resolution for the Snohomish River Estuary Project survey area:

- Average First Return Density = 6.97/m^2 (0.64/ft^2)
- Average Ground Point Density = 1.64/m^2 (0.15/ft^2)

Figure 4. Density distribution for first return laser points
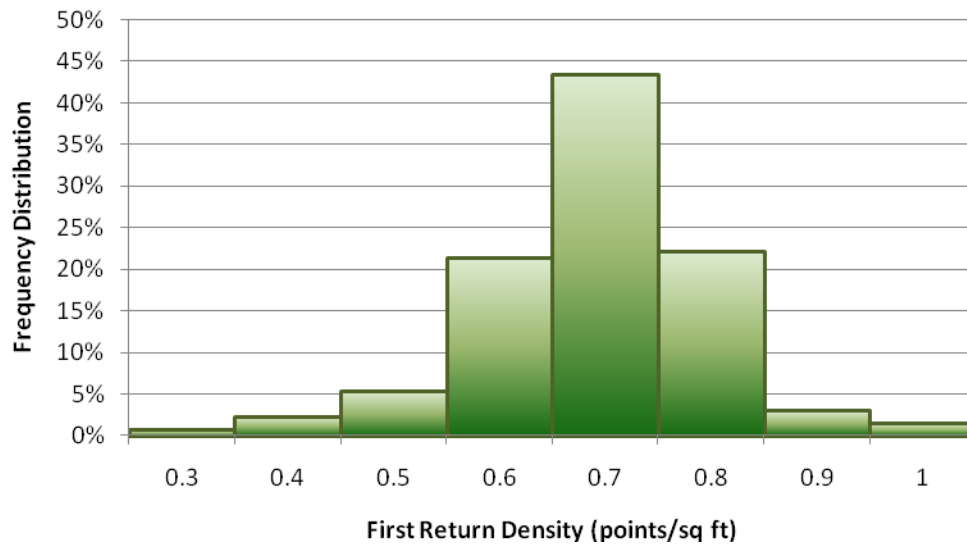
Figure 5. Density distribution for ground-classified laser points.
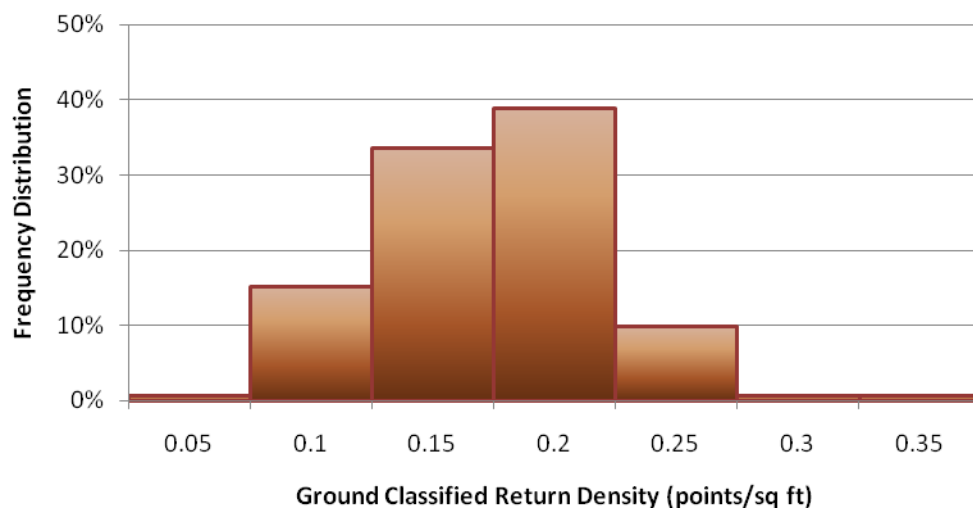
Figure 6. First return laser point density per 0.75' USGS Quadrangle.

First Return Density

points per square foot

- 0.28 - 0.45
- 0.46 - 0.58
- 0.59 - 0.67
- 0.68 - 0.77
- 0.78 - 0.98

0   1   2   4 Miles

LiDAR Data Acquisition and Processing: Snohomish River Estuary, WA

Prepared by Watershed Sciences, Inc.
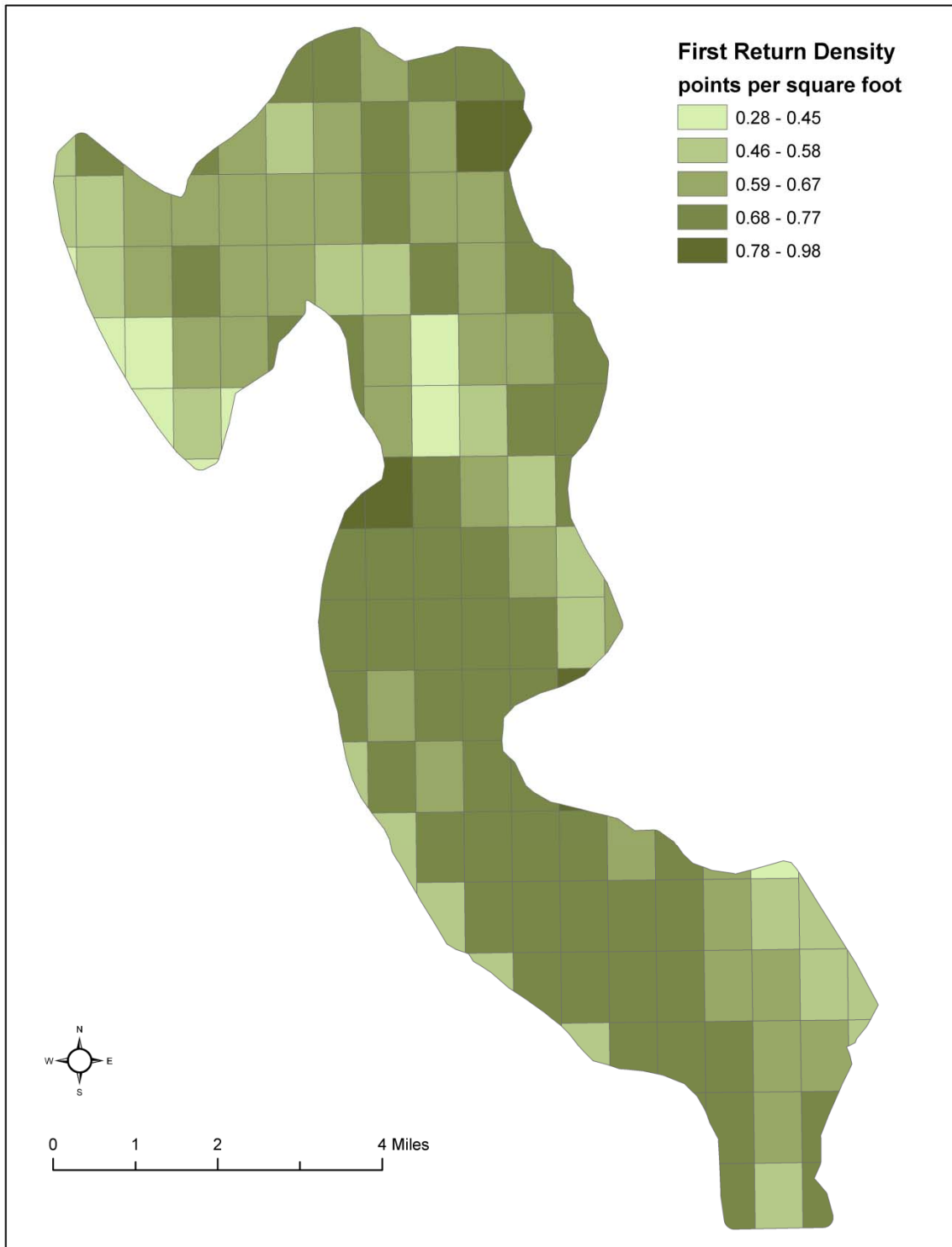
Figure 7. Ground-classified laser point density per 0.75' USGS Quadrangle.

Ground Classified Point Density
points per square foot

	0.05 - 0.10
	0.11 - 0.14
	0.15 - 0.17
	0.18 - 0.21
	0.22 - 0.31

0 1 2 4 Miles

LiDAR Data Acquisition and Processing: Snohomish River Estuary, WA

Prepared by Watershed Sciences, Inc.
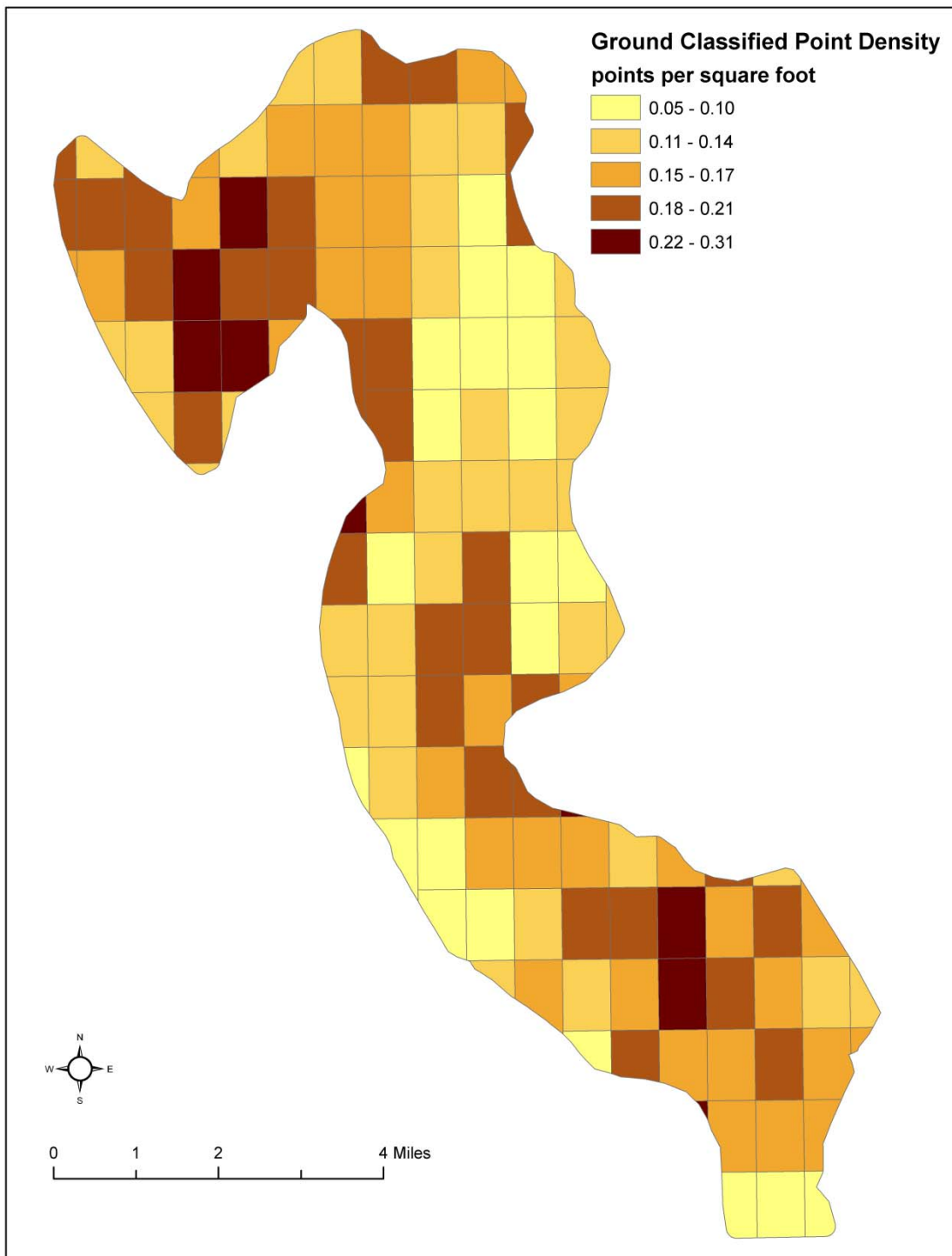
5.3 LiDAR Relative Accuracy Calibration Results

Relative accuracies for the Snohomish River Estuary Project survey area:

- o Project Average = 0.13 ft (.039 m)
- o Median Relative Accuracy = 0.13 ft (.039 m)
- o 1σ Relative Accuracy = 0.14 ft (.042 m)
- o 2σ Relative Accuracy = 0.15 ft (.046 m)

Figure 8. Distribution of relative accuracies per flight line, non slope-adjusted
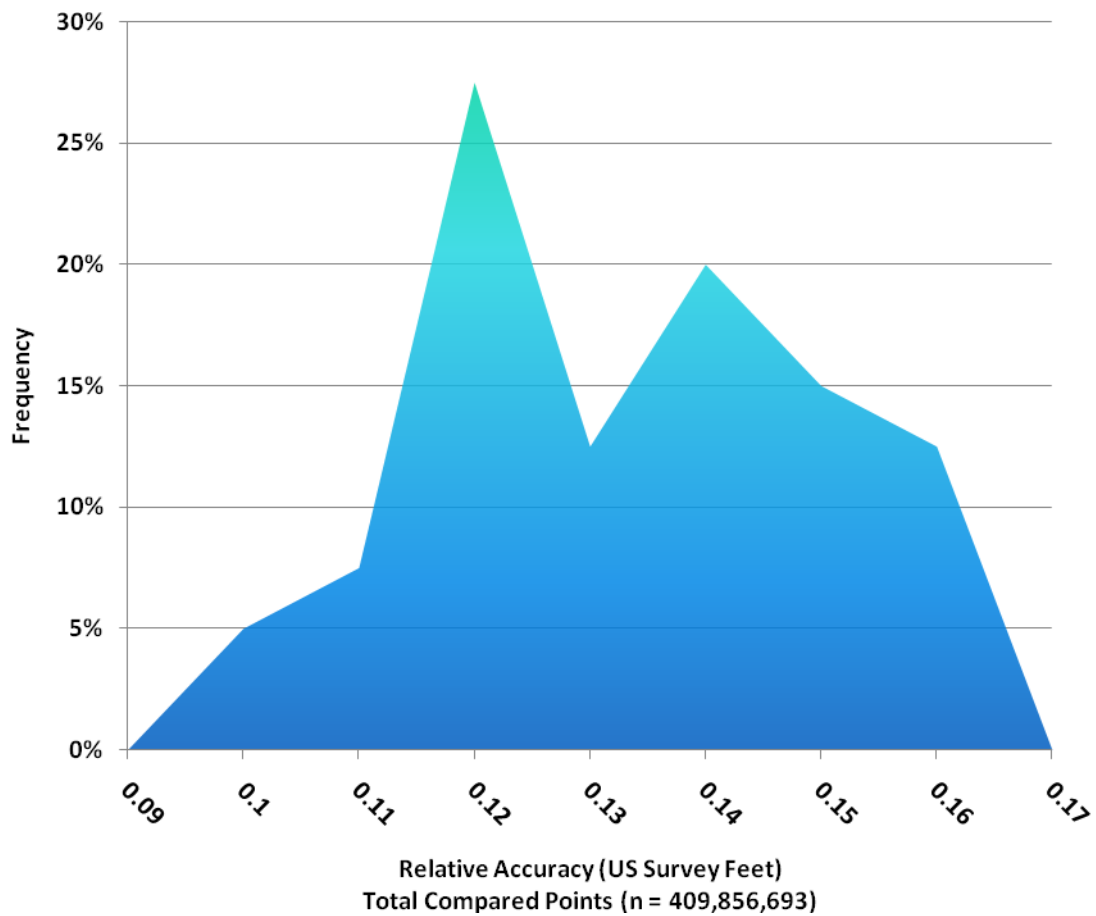
5.4 LiDAR Absolute Accuracy

Absolute accuracies for the Snohomish survey area

Table 4. Absolute Accuracy – Deviation between laser points and RTK survey points

RTK Surface Type	RTK Survey Sample Size (n)	Root Mean Square Error (RMSE)	Standard Deviations		Minimum Δz	Maximum Δz	Average Δz
			1 sigma (σ)	2 sigma (σ)			
Hard-surface (Watershed Sciences)	806	0.099 ft (0.03 m)	0.097 ft (0.03 m)	0.19 ft (0.057 m)	-0.29 ft (-0.087 m)	0.18 ft (0.055 m)	-0.055ft (-0.017 m)
Short Vegetation (Watershed Sciences)	188	0.40 ft (0.12 m)	0.19 ft (0.056 m)	0.80 ft (0.25 m)	-0.63 ft (-0.19 m)	2.0 ft (0.61 m)	0.20 ft (0.061 m)
Tall Vegetation (Client August)	249	0.93 ft (0.28 m)	0.86 ft 0.26 m	1.9 ft (0.56 m)	-2.1 ft (-0.65 m)	2.8 ft (0.84 m)	0.61 ft (0.19 m)
Tall Vegetation* (Client April)	857	0.86 ft (0.26 m)	0.78 ft (0.24 m)	1.6 ft (0.49 m)	-3.8 ft (-1.2 m)	2.8 ft (0.86 m)	0.41 ft (0.12 m)
Tall Vegetation (Client April: all RTK points)	875	1.8 ft (0.16 m)	0.80 ft (0.24 m)	1.9 ft (0.59 m)	-24 ft (-7.3 m)	15 ft (4.5 m)	0.52 ft (0.16 m)

*Eighteen check points were treated as outliers due to significant disagreement with both the LiDAR data and proximate check points from the same survey. Outlier points were possibly caused by poor GPS due to masking or interference during the April RTK survey. We calculated the accuracy statistics with outliers both included and excluded. The outlier RTK points were localized in two areas identified in **Figure 9**

Figure 9. Client RTK point locations collected in April, 2009 with areas of poor GPS highlighted in red

Figure 10. Absolute Accuracy - Histogram Statistics, based on 806 hard surface points.
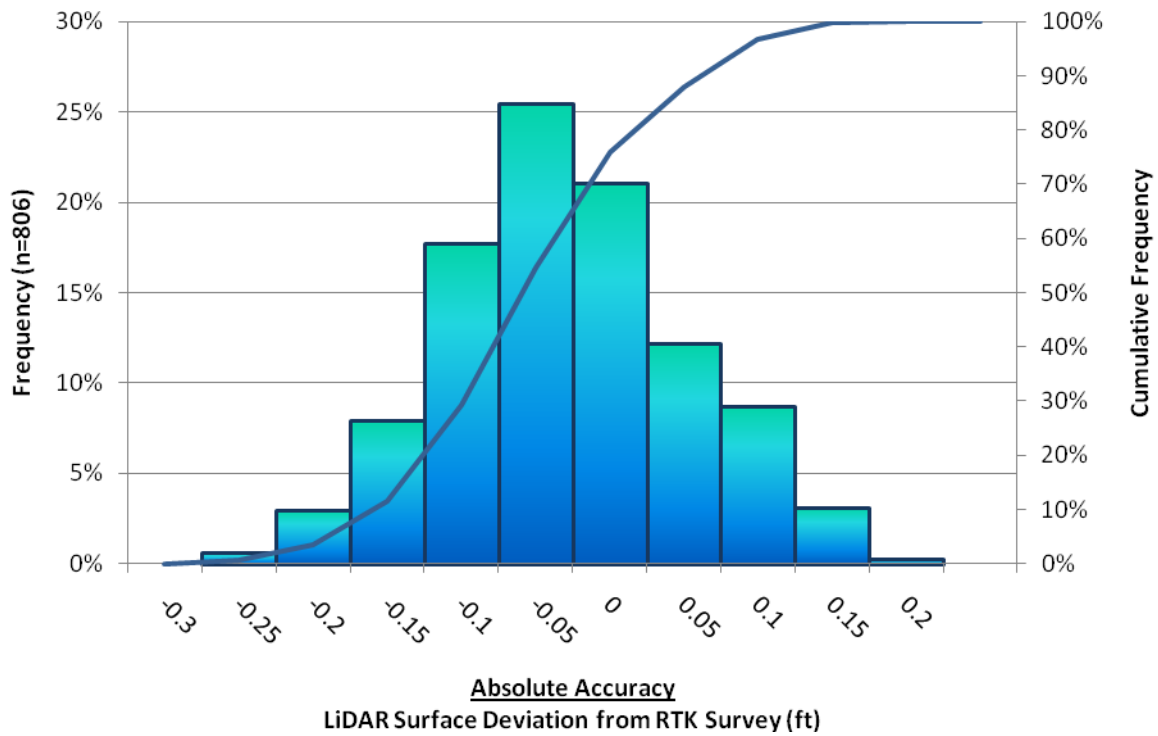
Figure 11. Absolute Accuracy – Absolute deviation, based on hard surface points.

LiDAR Data Acquisition and Processing: Snohomish River Estuary, WA

Prepared by Watershed Sciences, Inc.
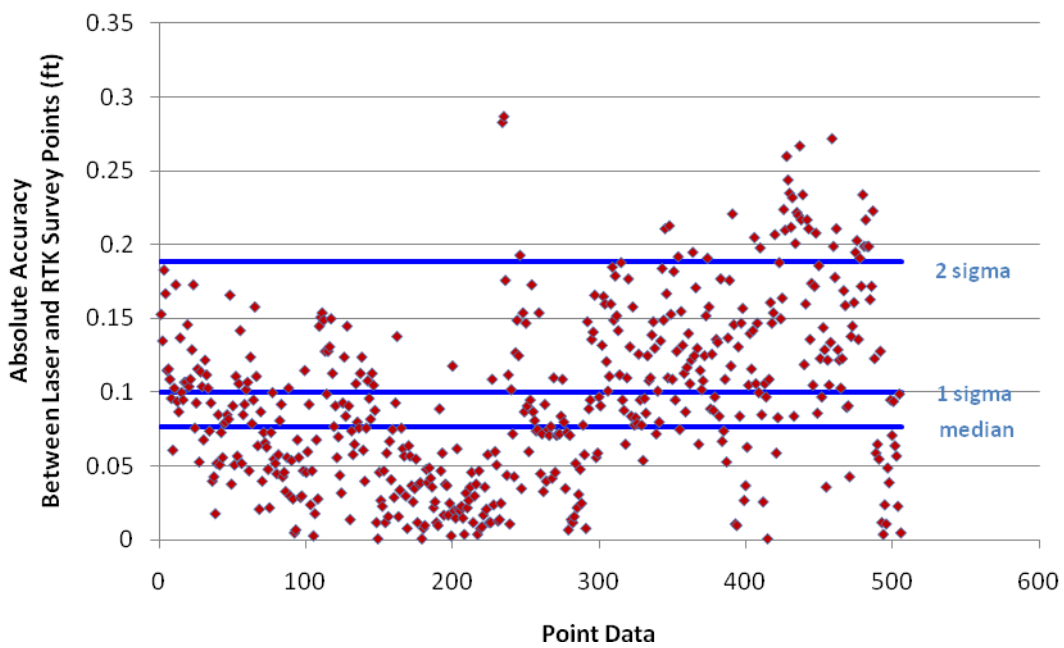
5.5 Photo delineation

Figure 12. Orthophoto tile delineation for the Snohomish survey area
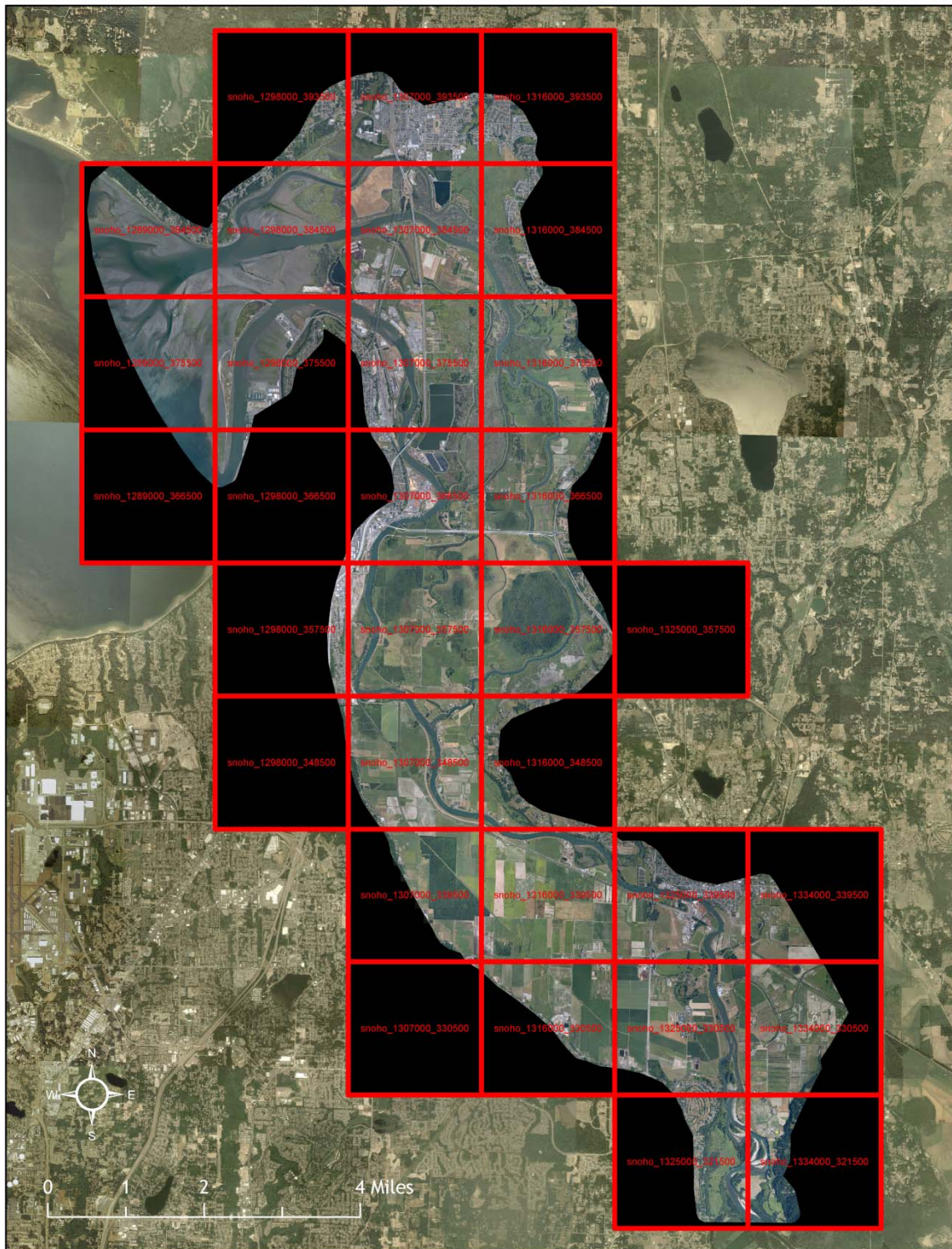
5.6 Photo Resolution and Accuracy

Table 5. Photo Resolution and Accuracy - Specifications and Achieved Values

	Targeted	Achieved
Resolution:	≤15 cm	23 cm (9 in)
Horizontal Accuracy (1 σ)	≤15 cm	1.6 cm

In order to capture the AOI under low tide conditions it was necessary to acquire the LiDAR at a higher elevation than would support 15 cm (6 in) photos. Instead the acquisition supported 9 in resolution imagery. Per discussions with Snohomish County, the photo resolution was secondary to tidal conditions.

Table 6. Deviation between aerial photos and intensity images

	Mean	Standard Deviation (1 Sigma)	Root Mean Square Error (RMSE)
Snohomish Survey Area	0.47 ft (0.14 m)	0.72 ft (0.22 m)	0.85 ft (0.26 m)

Figure 13. Checkpoint residuals derived from comparing aerial photos to intensity images; deviations are in feet.

5.7 Projection/Datum and Units

	Projection:	Washington State Plane FIPS 4601
Datum	**Vertical:**	NAVD88 Geoid03
	Horizontal:	NAD83
	Units:	U.S. Survey Feet

6. Deliverables

Point Data:	• All laser returns (LAS v. 1.2 format; 1/100th USGS quad delineation) • All laser returns (ASCII text format; 1/100th USGS quad delineation) • Ground classified points (ASCII text format; 1/100th USGS quad delineation)
Vector Data:	• Total Area Flown (shapefile format) • ¼ USGS quad delineation for (shapefile format) • 1/100 USGS quad delineation (shapefile format) • Photo tile delineation (shapefile format) • SBET Trajectories (ASCII text format)

Raster Data:	• Elevation models (3-ft resolution)
	  • Bare Earth Model (ESRI GRID format; 1/4th USGS quad delineation)
	  • Highest Hit Model (ESRI GRID format; 1/4th USGS quad delineation)
	• Intensity images (GeoTIFF format, 1.5-ft resolution, 1/100th USGS quad delineation)
	• True-color Orthophotographs (8-bit, tiled in GeoTiff format)

Data Report:	• Full report containing introduction, methodology, and accuracy

7. Selected Images

Figure 14. 3D view of the northeast corner of the Snohomish survey area derived from ortho-photographs.

Figure 15. 3D view of the mouth of the Snohomish River looking east, the top layer is true color ortho-photos, the middle layer is a highest-hit model, and the bottom layer is a bare-earth model.
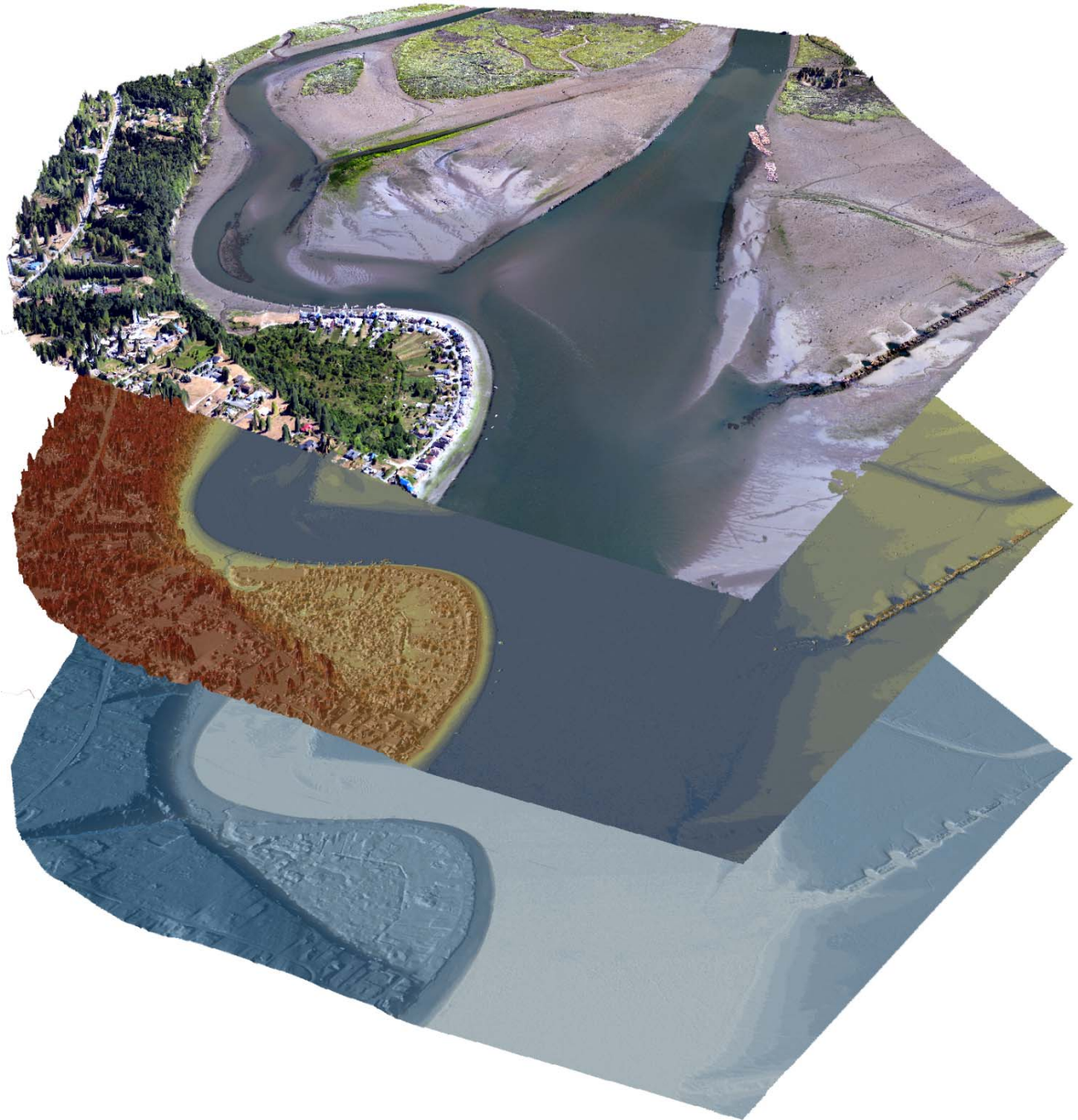
Figure 16. 3D view of Snohomish river derived from ortho photos.
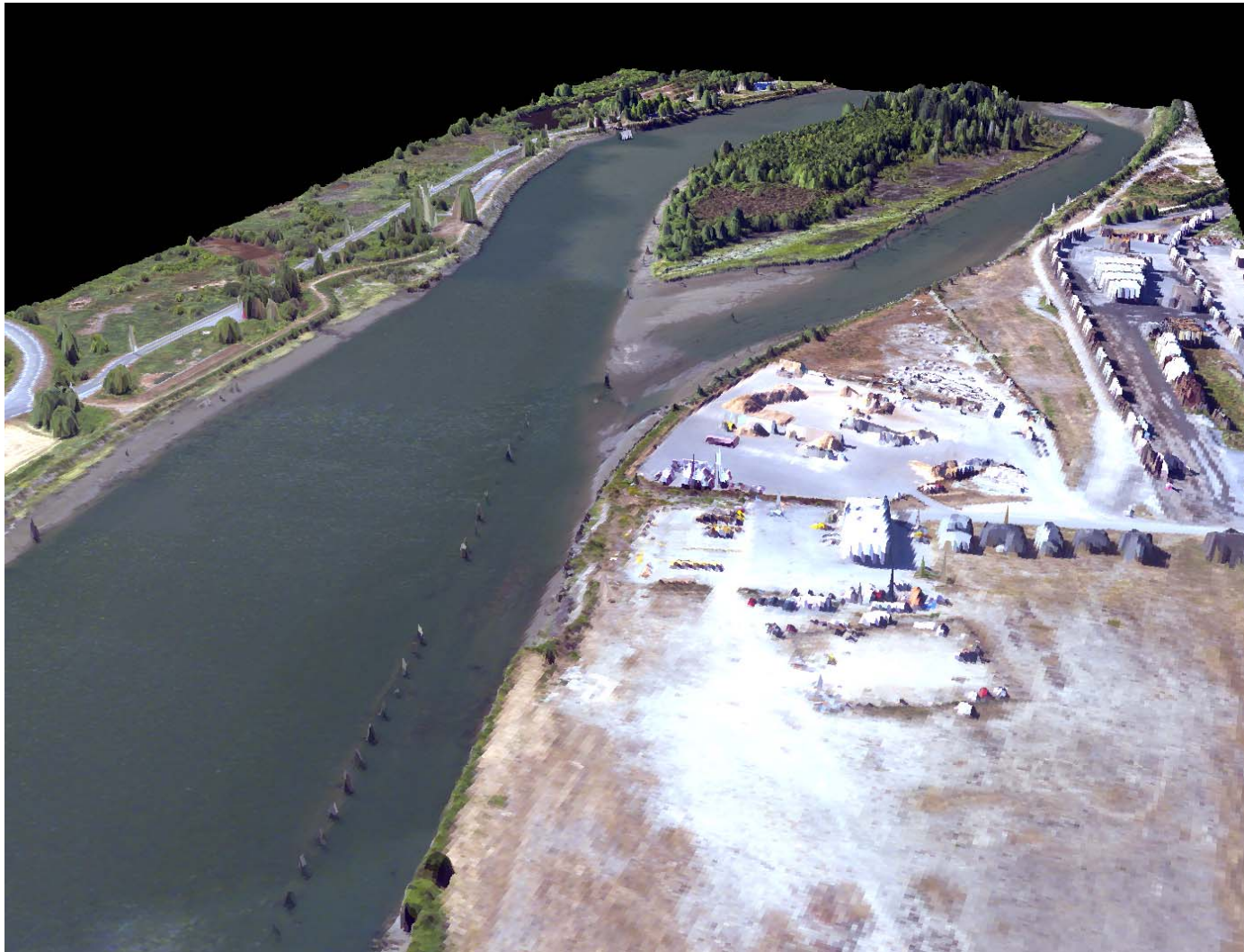
8. Glossary

1-sigma (σ) Absolute Deviation: Value for which the data are within one standard deviation (approximately 68th percentile) of a normally distributed data set.

2-sigma (σ) Absolute Deviation: Value for which the data are within two standard deviations (approximately 95th percentile) of a normally distributed data set.

Root Mean Square Error (RMSE): A statistic used to approximate the difference between real-world points and the LiDAR points. It is calculated by squaring all the values, then taking the average of the squares and taking the square root of the average.

Pulse Rate (PR): The rate at which laser pulses are emitted from the sensor; typically measured as thousands of pulses per second (kHz).

Pulse Returns: For every laser pulse emitted, the Leica ALS 50 Phase II system can record *up to four* wave forms reflected back to the sensor. Portions of the wave form that return earliest are the highest element in multi-tiered surfaces such as vegetation. Portions of the wave form that return last are the lowest element in multi-tiered surfaces.

Accuracy: The statistical comparison between known (surveyed) points and laser points. Typically measured as the standard deviation (sigma, σ) and root mean square error (RMSE).

Intensity Values: The peak power ratio of the laser return to the emitted laser. It is a function of surface reflectivity.

Data Density: A common measure of LiDAR resolution, measured as points per square meter.

Spot Spacing: Also a measure of LiDAR resolution, measured as the average distance between laser points.

Nadir: A single point or locus of points on the surface of the earth directly below a sensor as it progresses along its flight line.

Scan Angle: The angle from nadir to the edge of the scan, measured in degrees. Laser point accuracy typically decreases as scan angles increase.

Overlap: The area shared between flight lines, typically measured in percents; 100% overlap is essential to ensure complete coverage and reduce laser shadows.

DTM / DEM: These often-interchanged terms refer to models made from laser points. The digital elevation model (DEM) refers to all surfaces, including bare ground and vegetation, while the digital terrain model (DTM) refers only to those points classified as ground.

Real-Time Kinematic (RTK) Survey: GPS surveying is conducted with a GPS base station deployed over a known monument with a radio connection to a GPS rover. Both the base station and rover receive differential GPS data and the baseline correction is solved between the two. This type of ground survey is accurate to 1.5 cm or less.

9. Citations

Soininen, A. 2004. TerraScan User's Guide. TerraSolid.

Appendix A

LiDAR accuracy error sources and solutions:

Type of Error	Source	Post Processing Solution
GPS (Static/Kinematic)	Long Base Lines	None
	Poor Satellite Constellation	None
	Poor Antenna Visibility	Reduce Visibility Mask
Relative Accuracy	Poor System Calibration	Recalibrate IMU and sensor offsets/settings
	Inaccurate System	None
Laser Noise	Poor Laser Timing	None
	Poor Laser Reception	None
	Poor Laser Power	None
	Irregular Laser Shape	None

Operational measures taken to improve relative accuracy:
1. <u>Low Flight Altitude</u>: Terrain following is employed to maintain a constant above ground level (AGL). Laser horizontal errors are a function of flight altitude above ground (i.e., ~ $1/3000^{th}$ AGL flight altitude).
2. <u>Focus Laser Power at narrow beam footprint</u>: A laser return must be received by the system above a power threshold to accurately record a measurement. The strength of the laser return is a function of laser emission power, laser footprint, flight altitude and the reflectivity of the target. While surface reflectivity cannot be controlled, laser power can be increased and low flight altitudes can be maintained.
3. <u>Reduced Scan Angle</u>: Edge-of-scan data can become inaccurate. The scan angle was reduced to a maximum of $\pm 12^{o}$ from nadir, creating a narrow swath width and greatly reducing laser shadows from trees and buildings.
4. <u>Quality GPS</u>: Flights took place during optimal GPS conditions (e.g., 6 or more satellites and PDOP [Position Dilution of Precision] less than 3.0). Before each flight, the PDOP was determined for the survey day. During all flight times, a dual frequency DGPS base station recording at 1–second epochs was utilized and a maximum baseline length between the aircraft and the control points was less than 19 km (11.5 miles) at all times.
5. <u>Ground Survey</u>: Ground survey point accuracy (i.e. <1.5 cm RMSE) occurs during optimal PDOP ranges and targets a minimal baseline distance of 4 miles between GPS rover and base. Robust statistics are, in part, a function of sample size (n) and distribution. Ground survey RTK points are distributed to the extent possible throughout multiple flight lines and across the survey area.
6. <u>50% Side-Lap (100% Overlap)</u>: Overlapping areas are optimized for relative accuracy testing. Laser shadowing is minimized to help increase target acquisition from multiple scan angles. Ideally, with a 50% side-lap, the most nadir portion of one flight line coincides with the edge (least nadir) portion of overlapping flight lines. A minimum of 50% side-lap with terrain-followed acquisition prevents data gaps.
7. <u>Opposing Flight Lines</u>: All overlapping flight lines are opposing. Pitch, roll and heading errors are amplified by a factor of two relative to the adjacent flight line(s), making misalignments easier to detect and resolve.

LiDAR Data Acquisition and Processing: Snohomish River Estuary, WA

Prepared by Watershed Sciences, Inc.